Biochimica et Biophysica Acta, 987 (1989) 104–110
Elsevier

BBAMEM 74664

A description of the phospholipid arrangement intermediate to the humidity produced L_α and H_{II} phases in dioleoylphosphatidylcholine and its modification by dioleoylphosphatidylethanolamine as studied by X-ray diffraction

Jeremy P. Bradshaw [1,*], Michael S. Edenborough [2], Philip J.H. Sizer [1,**] and Anthony Watts [2]

[1] *Department of Biochemistry, University of Edinburgh Medical School, Edinburgh, Scotland, and* [2] *Department of Biochemistry, University of Oxford, Oxford (U.K.)*

(Received 29 May 1989)

Key words: Dioleoylphosphatidylcholine bilayer; Water/lipid system; Lamellar phase; Hexagonal H_{II} phase; Rippled phase; X-ray diffraction

X-ray diffraction from ordered multilayers has been used to study the structure of the lipid-water system in orientated multilayers of 1,2-dioleoyl-*sn*-glycero-3-phosphocholine (DOPC) at 30 °C as a function of water content. At high levels of water content the structure is lamellar (L_α), comprising equidistant lipid bilayers of constant thickness separated by layers of water. The low water content structure is a two-dimensional hexagonal array with narrow water channels (H_{II}). X-ray scattering density profiles are derived for both structures. The presence of a stable intermediate rippled structure between the L_α and H_{II} phases is demonstrated and a model is presented which involves a smooth structural transition between the two extremes described. The transition from L_α to H_{II} phase is related to the bilayer thickness and not to any other variable parameter such as water content or composition. The effect of 1,2-dioleoyl-*sn*-glycero-3-phosphoethanolamine (DOPE) on the structure and phase transition characteristics of the system is reported.

Introduction

Phospholipids are one of the major components of biological membranes and spontaneously form a wide variety of ordered structures with water. The particular structure adopted by such a system has been shown to be dependent on a number of factors, including temperature and water content [1]. If the temperature and water content are high enough the phospholipids are arranged in laterally-disordered lamellae. Lowering either water content or temperature generally causes the system to undergo a transformation into a new conformation in which the order extends in more than one direction. Ripples [2], hexagonal arrays [3] and constant mean curvature (CMC) surfaces [4] are examples of such structures. It is a feature of phospholipid-water systems that they can maintain a high degree of order in one direction whilst possessing little order in another plane. The exact relationship between the conformation of the different planes of three-dimensional order is not well understood.

The conformational transitions between the various morphological forms of phospholipid-water systems have been studied in great detail in a number of systems, and by a variety of techniques, including differential scanning calorimetry [5–7], X-ray diffraction [1,2], electron microscopy [8], electron spin resonance [9], nuclear magnetic resonance [10–12], fluorescence [13,14] and light scattering [15]. However, neither the nature of the intermediate structures between stable phases nor the effect of mixed phospholipid types on their formation have been fully elucidated. Moreover, although intermediate structures have been shown to be depen-

* Current address: Department of Preclinical Veterinary Sciences, University of Edinburgh, Summerhall, Edinburgh, EH9 1QH, Scotland, U.K.

** Current address: Evans Biologicals Ltd., Speke, Liverpool, L24 9GR, U.K.

Abbreviations: DOPC, 1,2-dioleoyl-*sn*-glycero-3-phosphocholine; DOPE, 1,2-dioleoyl-*sn*-glycero-3-phosphoethanolamine; PC, phosphatidylcholine; PE, phosphatidylethanolamine.

Correspondence: J.P. Bradshaw, Department of Preclinical Veterinary Sciences, University of Edinburgh, Summerhall, Edinburgh, EH9 1QH, Scotland, U.K.

dent on the nature of the acyl chain of the phospholipid [6], little is known about the influence of the headgroup region of the phospholipid, even though some lipid types have a greater propensity to form bilayer rather than hexagonal structures, and vice versa [16].

Although the lipid content of living cells can be extremely variable, some trends may be noted in the composition of membranes of mammals. Phosphatidylcholine is overall the most common phospholipid headgroup, and oleic acid represents the most frequently occurring fatty acid chain. The content of phosphatidylethanolamine also tends to be high in mammalian cells, particularly in the inner membrane of mitochondria. In this study the lamellar to hexagonal phase change induced by hydration level has been investigated in bilayers of phosphatidylcholine and phosphatidylethanolamine, both with oleic acid chains. The biological significance of the difference conformations of phospholipid-water systems has long been the subject of speculation. Whilst lamellar structures bestow a selectively permeable barrier to the volumes which they occlude, they also permit a certain degree of flexibility on the structure and freedom of motion of the individual lamellar components. Roles for the non-bilayer structures detected in natural membranes [17] in membrane fusion [18], in phospholipid translocation (flip-flop) from one monolayer to the other [19] and in the transport of proteins across the bilayer [20] have been described, and there is a certain amount of experimental evidence for there being a correlation between the structural phase of the phospholipid and the physiological properties of a membrane [21].

X-ray diffraction provides a suitable method for the study of the hydration dependent structural transformations of phospholipid systems. Most of the previous X-ray diffraction studies of phospholipid-water systems have used random dispersion samples. Much more information can be obtained if the sample is ordered on a substrate. An X-ray diffraction pattern from such an ordered system can be considered to be the product of two components. The first of these is the molecular transform and consists of the contribution to the diffraction pattern of the repeating unit within the diffracting structure. In the lipid-water systems of the present study this represents the electron density profile of a single lipid and water layer which constitutes the unit cell. The other component is the lattice transform, which corresponds to the geometric arrangement by which the repeating unit is assembled into the three-dimensional array of lipid molecules and water. In its simplest form, the lattice transform consists of a row of points on the normal to the plane of a multilayer system of planar lamellae. In this present study we have utilised the information contained in both components of the diffraction pattern in an attempt to elucidate the nature of the conformational transition, induced by changing the water content of the system, from planar bilayers to hexagonal arrays of cylindrical micelles.

Materials and Methods

Sample preparation

The phospholipids 1,2-dioleoyl-*sn*-glycero-3-phosphocholine (DOPC) and 1,2-dioleoyl-*sn*-glycero-3-phosphoethanolamine (DOPE) were obtained from Sigma and confirmed to be single species by thin-layer chromatography before use. Highly orientated multilayers were prepared by spreading $6 \cdot 10^{-6}$ mol (about 5 mg) of phospholipid in chloroform over a curved glass (10–20 mm radius) substrate. The solvent was allowed to evaporate under a stream of warm air and the sample was fully dried under vacuum for 24 h. The lipid was hydrated by annealing it for at least 4 h at 70°C and 100% humidity. All samples were run at 30°C, after being allowed to equilibrate at this temperature for 1 h in the sample cell. Three types of sample were prepared in this way, pure DOPC, DOPC with 10% (mol/mol) DOPE and DOPC with 30% (mol/mol) DOPE.

X-ray diffraction

During the diffraction experiment the samples were held in a purpose built environmental cell which allowed the temperature and humidity to be closely controlled. The cell contained a small boat of saturated salt solution. The choice of salt and temperature controlled the humidity inside the specimen cell. The relative humidity produced by each set of parameters was determined by duplicating the experimental conditions in a sealed dessicator containing a hydrometer. A dehydrated environment was achieved by replacing the saturated salt solution with phosporus pentoxide (P_2O_5), and a saturated environment with water. In the camera used to produce the diffraction patterns, 0.3 mm collimated, Nickel filtered radiation from a Marconi-Elliot GX-13 rotating anode X-ray generator was scattered by the sample onto a pack of four 13×18 cm films positioned 175 mm away. The diffracted beam path was evacuated to reduce background noise from air-scattered radiation. The developed films were scanned on a Joyce Loebl Chromoscan 3 Microdensitometer. The position of each diffraction peak was recorded and an iterative least-squares refinement programme was used to calculate the lattice parameters of each sample.

Corrections

Before the diffracted intensities could be used in the form of structure factors to calculate the electron density distribution normal to the bilayer surface of each sample, a number of corrections were applied.

(1) Background. The background optical density level, corresponding to incoherent X-ray scatter and pigments in the X-ray film base, was subtracted from each dif-

fracted intensity. This was achieved by measuring the optical density of each film in the region immediately adjacent to a peak and interpolating across its base. This value was then subtracted from the peak. After correcting for this factor the diffracted intensities were determined by integrating the area under each peak.

(2) Lorentz factor. This factor is applied to each reflection, and takes into account the spreading out of the intensity in reciprocal space due to the disorientation of the bilayers in the specimen. The nature of the correction factor is dependent on the camera geometry and has been described by Franks and Lieb [23].

(3) Absorption. A correction was applied to allow for absorption of the diffracted radiation by the lipid film. This factor, as described by Franks [24], is a function of the Bragg angle. The largest correction was applied to the first order of diffraction from the fully hydrated sample, its intensity being increased by a factor of 1.3.

Phasing the reflections

In order to calculate the electron density across each bilayer it was necessary to determine the phase of each structure factor. The phase of a diffraction peak from a centrosymmetric unit cell may only be in phase, or 180° out of phase, with respect to another peak. The convenient notation of + or − may be used to indicate whether the phase of a particular structure factor is 0° or 180°. The method employed to determine the phases is based on the observation that the final electron density distributions of a swelling series of bilayers will differ from each other only in the width of the water region [25]. Therefore, the phases of the diffracted rays were determined by observation of changes with hydration. This search is facilitated by using any other information which puts constraints upon the expected structure. In our case the structure of the same bilayer system, at two hydration levels, had already been solved by neutron diffraction [22]. Although there are differences between the electron and neutron scattering profiles these differences are neither substantial nor unpredictable [26].

Results

X-ray diffraction pattern

The X-ray diffraction from assemblies of DOPC falls into three well defined patterns depending on hydration. At high humidities (Fig. 1) the pattern consists of well-resolved, on-axis peaks corresponding to the lattice transform of the fundamental lamellar bilayer repeat with unit periodicity. From measurements of the spacing of these peaks it is possible to calculate D, the bilayer repeat distance, which represents the width of one complete phospholipid bilayer and the thickness of one water layer. At lower humidities an additional set of diffraction intensities arises. These intensities are situated close to each bilayer peak, on both sides of the

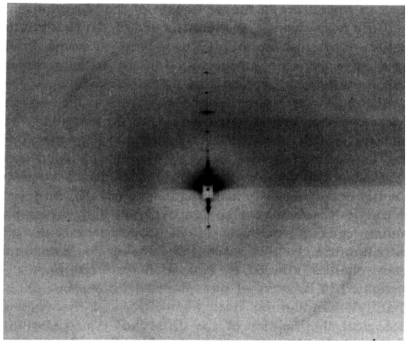

Fig. 1. The low-angle region of the X-ray diffraction pattern produced by ordered lamellar multibilayers of DOPC. Eight orders of the lamellar diffraction intensity may be seen on the meridian. The large rings visible in the diffraction pattern (and also in Figs. 2 and 3) are artifactual, and are caused by X-rays scattered by the mylar windows of the specimen chamber.

axis. In the example shown in Fig. 2 these off-axis peaks are strongest at the sides of the first and fourth orders of the lamellar diffraction peak. At even lower humidities yet another series of diffraction peaks co-exists with the other two sets of peaks, indicating that the bilayer system has transformed into the hexagonal H_{II} phase

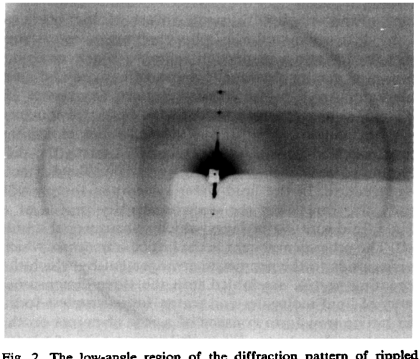

Fig. 2. The low-angle region of the diffraction pattern of rippled multibilayers of DOPC containing 10% (mol/mol) DOPE at 36% relative humidity. The off-meridional diffraction peaks which are not from a hexagonal phase are strongest to each side of the first- and fourth-order lamellar diffraction intensities.

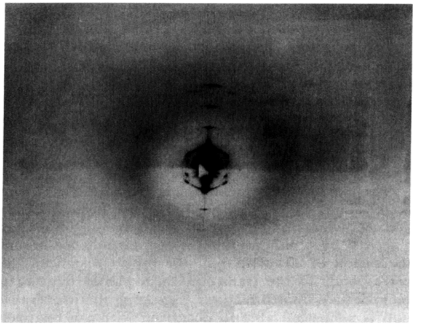

Fig. 3. The low-angle region of the diffraction pattern of DOPC at 0% relative humidity. The distribution of diffraction peaks is quite different to those observed Figs. 1 and 2. The speckled appearance of the diffraction intensities is caused by the coexistence within the sample of a number of discrete domains of phospholipid and water.

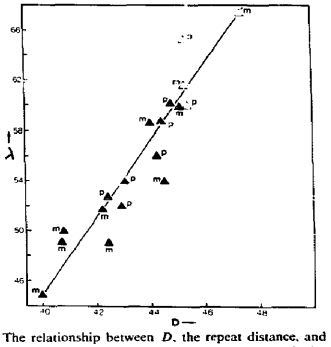

Fig. 5. The relationship between D, the repeat distance, and λ, the wavelength of the rippled phase (▲) and the repeat for the hexagonal phase (▲). Each point represents a single experimental observation. Points labelled with the latter 'p' were obtained from preparations of pure DOPC and those indicated with 'm' were obtained from mixtures of DOPC and DOPE. All units are Ångstroms.

(Fig. 3). Similar diffraction patterns were obtained from samples containing 10 or 30% (mol/mol) DOPE.

Bilayer spacing

The measured lattice parameters are summarised graphically in Figs. 4 and 5, which show the relationships between relative humidity and bilayer repeat distance and between bilayer repeat distance and ripple wavelength, respectively. There is a discontinuity between D for the lamellar phase and the hexagonal phase. The dependence on D for the hexagonal and intermediate phases is the same for each phase with relative humidity.

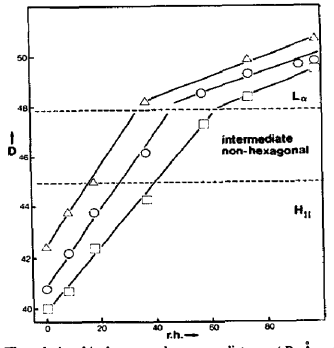

Fig. 4. The relationship between the repeat distance (D, Ångstroms), and relative humidity (r.h., %) at 30°C. △, pure DOPC; ○, DOPC with 10% (mol/mol) DOPE; □, DOPC with 30% (mol/mol) DOPE. Each point represents the mean of between two and six samples. The dashed lines indicate the regions of structural transition between (top) lamellar and rippled bilayers and (bottom) between rippled bilayer and hexagonal phase.

Bilayer profiles

The X-ray scattering profiles for lipid assemblies at a range of relative humidities were calculated from the corrected intensities and derived phases. These scattering profiles shown in Fig. 6 correspond to the projection of the electron density distribution onto the normal to the bilayer surface. The plots are aligned horizontally to superimpose the centre of each lipid bilayer, and displaced vertically for clarity. The peak of each profile reflects the position of the electron-dense phosphate groups of the phospholipid, whilst the trough towards the centre of the bilayer is due to the terminal methyl groups of the fatty acyl chains.

Discussion

Bilayer profiles

With increased humidity the electron density profile of DOPC expands anisotropically in the direction parallel to the long molecular phospholipid axis. The region of expansion is restricted to the area which represents the water layer. There is no appreciable difference in X-ray scattering profile at high humidity between the bilayers containing DOPE and those of pure DOPC.

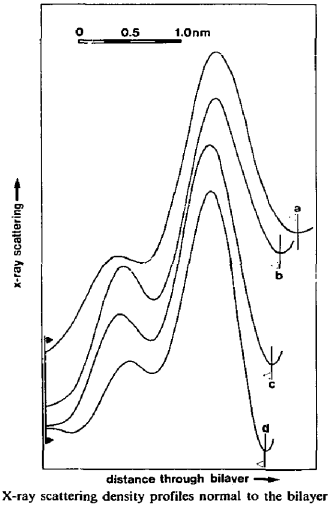

Fig. 6. X-ray scattering density profiles normal to the bilayer across half a DOPC bilayer at 30 °C. The vertical scale represents relative electron density (arbitrary scale) and the horizontal scale is distance across the bilayer or, in the case of the hexagonal phase, (line d) distance along the vertical line separating the centres of two water channels. In each case half of each centrosymmetric unit cell is shown. (a) 98% relative humidity, (b) 37%, (c) 18%, (d) 0%. The profiles have been displaced vertically to prevent superposition of the curves.

This observation can be explained by the similarity in X-ray scattering characteristics of the atoms C, N and O, making the PC headgroup indistinguishable from the surrounding water. It is interesting to note that apart from the contraction of the water layer, there does not appear to be any significant change in the electron scattering profile between the two phases studied. There can be, therefore, no large conformational change in the molecular structure of the phospholipid in the transition from L_α to H_{II}, as confirmed by the samll values of H for the thermally reduced bilayer to H_{II} transition [27].

The nature of the phase transition

The L_α to H_{II} phase transition appears to occur in two stages. Intermediate to the liquid crystalline phase and the hexagonally packed H_{II} phase, the lipid system takes another form. The lack of a second order of the intermediate phase reflection even after extensive overexposure of the films suggests that the phase is a sinusoidal ripple, since the sine function can be fully described in Fourier transformation by a single order. This contrast with the $P_{\beta'}$ ripple observed as the transitional form between $L_{\beta'}$ and L_α phases in dimyristoyl and dipalmitoyl lipid-water systems, which is not sinusoidal [2]. The lack of three-dimensional (h, k, l) reflections and the observation of only two-dimensional sharp reflections indicate that the ripple is at least 100 nm deep and precise quantitation is outside the range of the experimental methods described here.

The non-rippled to rippled bilayer transition

The experimental information given in Fig. 4 suggests a biphasic relationship between bilayer thickness and relative humidity (Fig. 4). This relationship is characterised by a discontinuity in the dependence around the region of $D = 4.75$ nm, the repeat distance. This corresponds to the transition from planar bilayers to intermediate rippled bilayers, indicating that this transition is somewhat abrupt, occurring within a relatively small humidity range. The abruptness of this transition suggests a degree of co-operativity between neighbouring phospholipids producing a concerted change in molecular arrangement triggered by the alteration in hydration level. It is interesting to note that the point of transition is related to bilayer thickness, and not relative humidity, as shown by the observation that the transition occurs at the same value of D irrespective of DOPE content in the bilayer.

The rippled bilayer to hexagonal transition

The transition from rippled bilayer to hexagonal phase occurs when the bilayer thickness is in the region of 4.5 nm. In contrast to the abrupt well defined transition from non-rippled bilayer to rippled bilayer this transformation appears to be broader, though this appearance may be due to the limited number of data points available. As the relative humidity decreases, the X-ray diffraction patterns (see Figs. 2 and 3) show that the first-order ripple reflection changes into the first-order hexagonal reflection without a change in the dependence of ripple wavelength on D repeat or changing the ripple shape. Determination of the repeat distance, shown in Figs. 4 and 5 do not exhibit a distinct transition point between the rippled bilayer and hexagonal states. The relationship between D-repeat and ripple wavelength or hexagonal repeat (Fig. 5) seems to be linear, and not related to either humidity or DOPE content. This suggests that the cylinder diameter in the H_{II} phase and the bilayer ripples have the same dimensions. Fig. 7 shows a possible model to explain the observations. As the humidity decreases the wavelength of the ripple also decreases. The combined effect of reducing the ripple wavelength and D-repeat produces 'pockets' of water connected by narrow water courses. Reducing the humidity still further causes the disappearance of these water courses. Slight rearrangement of the lipids around each triangular prismatic water pocket

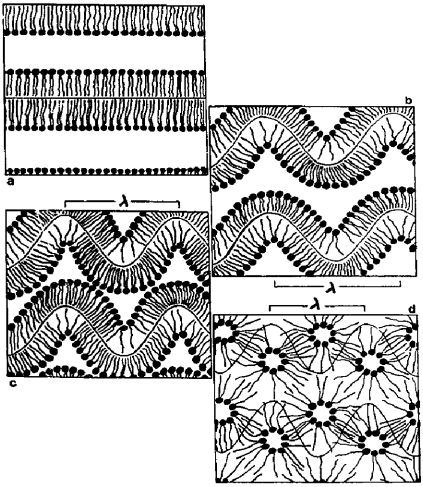

Fig. 7. A model of the L_α to H_{II} phase transition of DOPC which fits the experimental observations described in the text. The vertical distance between the solid lines represents D, the unit repeat normal to the bilayer. At high humidities (over 70%) the phospholipids are arranged in planar bilayers (a). With decreasing hydration, the bilayer repeat distance drops below 4.75 nm, and the bilayer forms sinusoidal ripples (b) of wavelength λ. As the repeat distance continues to fall the rippled bilayers come closer together until they meet, causing the continuous water layers to break up into triangular prismatic water channels. The bilayers are close to this point in (c). Rearrangement of the phospholipids around these water channels gives the hexagonal H_{II} phase (d).

as shown in Fig. 7, possibly involving electrostatic interactions of the head-groups, produces the H_{II} packing, without altering the sinusoidal symmetry of the system.

Diffraction patterns collected from the less humid samples tended to have their diffraction peaks split up into many discrete dots, in the fashion of powder diffraction spots (see Fig. 3). This may be interpreted as indicating that the continuous uniform samples had broken down into discrete molecular domains coexisting within the sample. The dimensions of the diffraction dots can be used to estimate that the size of each domain is greater than 200 nm. The degree of orientation of these domains relative to each other is comparable to the mosaic spread of the homogeneous samples, since all the discrete spots comprising each diffraction peak superimpose the area occupied by the same peak in an isotropic sample.

The effect of the PE headgroup

The mixed DOPC and DOPE bilayers do not form a rippled phase at relative humidities above 70%. The increasing amounts of DOPE in the DOPC bilayers reduce the repeat distance of the system for any given humidity. This effect is observed at all relative humidities down to 0%, where the minimum thickness of the system is reduced from 4.24 nm with no DOPE to 4.00 nm with 30% DOPE. These values correlate well with neutron diffraction studies of the same systems [22]. This observation could be related to the lower hydration level of DOPE compared to DOPC, or could be a simple stereochemical phenomenon. The neutron diffraction studies have shown that increased molar percentages of DOPE with a smaller polar headgroup than DOPC allow the PC headgroup to lie closer to the bilayer surface. This would allow two bilayers to come nearer to each other, thus reducing the observed D-repeat. Since the presence of the rippled phase, and its wavelength, appear to be a function of the bilayer spacing, then any factor which causes a decrease in bilayer spacing may, as a secondary effect, also increase the humidity thresholds below which the ripple and H_{II} phases occur.

Another factor may also be contributing to the narrowing of the bilayers. Whilst the majority of the phospholipid headgroups may be indirectly linked through hydrogen bonding to surface water molecules [28,29], strong direct intermolecular PE-PE hydrogen bonds may exist. Such associations within bilayers containing DOPE would imply a lower level of hydration at a particular humidity and, in addition, encourage the formation of non-bilayer phases.

Acknowledgements

We thank Mr. K.C. Duff for technical assistance. P.J.H.S. was in receipt of a Resarch Fellowship from the University of Edinburgh Faculty of Medicine.

References

1 Luzzati, V. (1968) in Biological Membranes (Chapman, D., ed.), p. 71, Academic Press, New York.
2 Alecio, M.R., Miller, A. and Watts, A. (1985) Biochim. Biophys. Acta 815, 139.
3 Stoeckenius, W. (1962) J. Cell. Biol. 12, 221.
4 Thomas, E.L., Anderson, D.M., Henkee, C.S. and Hoffman, D. (1988) Nature 334, 598
5 Janiak, M.J., Small, D.M. and Shipley, G.G. (1976) Biochemistry 15, 4575.
6 Stumpel, J., Eibl, H. and Nicksch, A. (1983) Biochim. Biophys. Acta 727, 246.
7 Epand, R.M. and Bryzewska, M. (1988) Biochemistry 27, 8776.
8 Stoeckenius, W. (1962) J. Cell. Biol. 12, 221.
9 Marsh, D. and Watts, A. (1981) in Liposomes: From Physical Structure to Therepeutic Applications (Knight, C.G., ed.), Elsevier/North Holland Biomedical Press, Amsterdam.

10 Seelig, J. and Seelig, A. (1980) Q. Rev. Biophys. 13, 19.
11 Thayer, A.M. and Kohler, S.J. (1981) Biochemistry 20, 6831.
12 Siminovitch, D.J., Jeffrey, K.R. and Eibl, H. (1983) Biochim. Biophys. Acta 727, 122.
13 Lee, A.G. (1975) Biochim. Biophys. Acta 413, 11.
14 Suurkuusk, J., Lentz, B.R., Barenholz, R.L. and Thompson, T.E. (1976) Biochemistry 15, 1393.
15 Marsh, D., Watts, A. and Knowles, P.F. (1977) Biochim. Biophys. Acta 465, 500.
16 De Kruijff, B., Cullis, P.R., Verkleij, A.J., Hope, M.J., Van Echteld, C.J.A., Taraschi, T.F., Van Hoogevest, P., Killian, J.A., Rietveld, A. and Van de Steen, A.T.M. (1985) in Progress in Protein-Lipid Interactions (Watts, A. and De Pont, J.J.H.H.M., eds.), p. 89, Elsevier/North Holland, Amsterdam.
17 Corless, J.M. and Costello, M.J. (1981) Expt. Eye. Res. 32, 217.
18 Verkleij, A.J., Van Echteld, C.J.A., Gerritsen, W.J., Cullis, P.R. and De Kruijff, B. (1980) Biochim. Biophys. Acta 600, 620.
19 Noordam, P.C., Van Echteld, C.J.A., De Kruijff, B. and De Gier, J. (1981) Biochim. Biophys. Acta 646, 483.
20 Rietveld, A. and De Kruijff, B. (1984) J. Biol. Chem. 95, 487.
21 Ranck, J.L., Mateu, L., Sadler, D.M., Tardieu, A., Gulik-Krzywicki, T. and Luzzati, V. (1974) J. Mol. Biol. 85, 249.
22 Bradshaw, J.P., Edenborough, M., Sizer, P.J.H. and Watts, A. (1989) Biochemistry, submitted.
23 Franks, N.P. and Lieb, W.R. (1979) J. Mol. Biol. 131, 469.
24 Franks, N.P. (1976) J. Mol. Biol. 100, 345.
25 Torbet, J. and Wilkins, M.H.F. (1976) J. Theor. Biol. 62, 447.
26 Franks, N.P. and Lieb, W.R. (1981) in Liposomes: From Physical Structure to Therapeutic Applications (Knight, C.G., ed.), p. 243, Elsevier/North Holland Biomedical Press, Amsterdam.
27 Seddon, J.M., Cevc, G. and Marsh, D. (1983) Biochemistry 22, 1280.
28 Hauser, H., Pascher, I., Pearson, R.H. and Sundrell, S. (1981) Biochim. Biophys. Acta 650, 21.
29 Sixl, F. and Watts, A. (1983) Proc. Natl. Acad. Sci. USA 80, 1613.